



10th CIRP Sponsored Conference on Digital Enterprise Technologies (DET 2021) – Digital Technologies as Enablers of Industrial Competitiveness and Sustainability

Design and additive manufacturing of a fatigue-critical aerospace part using topology optimization and L-PBF process

Akin Dagkolu^{a,b,*}, Istemihan Gokdag^a, Oguzhan Yilmaz^b

^aTurkish Aerospace Industries Inc., Fethiye Mh. Havacılık Blv. No:17 06980 Ankara/Turkey

^bAdvanced Manufacturing Technologies Research Group, Faculty of Engineering, Gazi University, Celal Bayar Blv, 06570, Maltepe, Ankara/Turkey

* Corresponding author. E-mail address: akin.dagkolu@gazi.edu.tr

Abstract

Additive Manufacturing (AM) is a new generation manufacturing method and AM is using digital CAD data directed to the machine to manufacture. AM is therefore regarded as a direct digital manufacturing method. This research work presents the methodology for designing critical aerospace parts used under fatigue conditions for AM. Selected fatigue critical aerospace part was topologically optimized then re-designed for manufacturability. With this optimization study, 45 % mass saving was obtained while mechanical requirements were satisfied. Manufacturing simulations for thermal distortions are covered and the optimized part was manufactured with laser powder bed fusion (L-PBF) and secondary operations were applied.

© 2021 The Authors. Published by Elsevier B.V.

This is an open access article under the CC BY-NC-ND license (<http://creativecommons.org/licenses/by-nc-nd/4.0/>)

Peer-review under responsibility of the scientific committee of the 10th CIRP Sponsored Conference on Digital Enterprise Technologies (DET 2020) – Digital Technologies as Enablers of Industrial Competitiveness and Sustainability.

Keywords: Additive manufacturing; Selective laser melting; Topology optimization; Holistic process; Fatigue critical

1. Introduction

The aviation and space industries are the most critical sectors where additive manufacturing (AM) is most potentially used and the total revenues from AM are expected to gradually increase over the next 20 years [8]. Such an extraordinary trend of AM is of course the AM Technologies is regarded as the novel direct digital manufacturing (DDM). DDM defines as the de-centralized manufacturing of the parts in accordance with proper qualification and certification [5]. Another reason behind the extensive usage of AM can be correlated with the flexibility in design. Owing to the manufacturing freedom of the AM processes, more complex geometries having lighter and stiffer properties can be designed and manufactured. In design for AM, topology optimization (TO) method has been preferred due to its significant role in weight reduction.

Topology optimization is a mathematical method that determines the optimum material distribution under defined loading and boundary conditions within a specified design space [2]. Initial TO formulation that enables to find optimum shape and material distribution during the design of a structural part was

proposed as a seminal work [1]. Many contributions such as stress constraint and filters to deal with the numerical problems during design have been made to improve TO formulations using the initial methodology [4, 15]. In the aerospace industry, where designs are expected to be lightweight and high in strength, many components have been designed with the frequently used topology optimization method, such as pylons, ribs, and brackets [20, 7, 13]. Besides, the reason why topology optimization is used so frequently is it can offer a design solution for aerospace parts that are subjected to static, dynamic, and thermo-elastic loads [17, 14, 9]. In addition, the fact that the difficulties brought by the production method of the designed part (i.e. as draw direction, symmetry plane, and overhang angle) can be integrated into the optimization process as a constraint improves the design processes [18, 19]. Fatigue is considered as a constraint during the design to meet all the requirements since the structural parts used in aerospace applications are commonly under cyclic loads in service. During the design of a fatigue critical part, crack states of initiation caused by shear stress and propagation caused by normal stress should be investigated and the critical stress levels must be lower than allowable stresses. Constraints of high cycle fa-

2351-9789 © 2021 The Authors. Published by Elsevier B.V.

This is an open access article under the CC BY-NC-ND license (<http://creativecommons.org/licenses/by-nc-nd/4.0/>)

Peer-review under responsibility of the scientific committee of the 10th CIRP Sponsored Conference on Digital Enterprise Technologies (DET 2020) – Digital Technologies as Enablers of Industrial Competitiveness and Sustainability.

10.1016/j.promfg.2021.07.037

tigue(HCF) stress and static stress aggregated by modified p-norm were implemented to the TO problem formulation with the objective function of minimizing mass used for the conceptual design process of the lightweight structures [6]. Static analysis instead of costly dynamics analysis was performed to determine fatigue behavior using the modified-Goodman criterion. Relaxed equivalent stresses calculated with the Sines approach and the compliance constraint were integrated into the TO formulation [3]. The method which works fatigue damage for HCF was proven the applicability to the additively manufactured parts by numerical examples solved using two alloy steels [16]. In this study, a methodology for the design of a fatigue-critical aerospace part for AM is presented. The proposed methodology aiming to improve the fatigue behavior and stiffness per mass ratio includes modeling for additive manufacturing using TO, re-design, and analytical calculations using results of Finite Element (FE) analyses to determine the life cycles for the cyclic loadings containing HCF and low cycle fatigue (LCF).

2. Materials and Methods

2.1. Materials

The sample part was originally manufactured from annealed Ti-6Al-4V material with computer numerical control (CNC) machining process. The part is under variable loading in service for an aerospace application. To be able to use similar material properties, gas atomized Ti-6Al-4V (grade-5) powder is used in the additive manufacturing of the optimized part. The chemical composition of the Ti-6Al-4V powder supplied by the manufacturer is given in Table 1. This Ti alloy is frequently used in aerospace applications where high mechanical strength and fatigue resistance is needed. In this alloy, aluminum acts as α stabilizer and vanadium as β stabilizer [11].

Table 1. Chemical composition of the Ti-6Al-4V powder

Element	Al	V	O	N	C	H	Fe
	5,5-6,75	3,5-4,5	2000	500	800	150	3000
	wt.-%	wt.-%	ppm	ppm	ppm	ppm	ppm

2.2. Additive Manufacturing

All the samples and the optimized part were manufactured by laser powder bed fusion process (L-PBF) and using the EOSINT M280 machine. Manufacturing parameters were selected as the default parameter set for Ti-6Al-4V alloy supplied by the machine manufacturer and they are given in Table 2. The selected parameter set is held constant through all the works.

Table 2. L-PBF Manufacturing Parameters

Laser Power (W)	Scanning Speed (mm/s)	Hatch Distance (mm)	Layer Thickness (mm)
170	1250	0,015	0,03

Mechanical properties of the used Ti-6Al-4V alloy powder and the machine performance were validated after manufacturing of test samples and testing them according to the standards such as ASTM E8, E23, E466.

2.3. Post Processes

All of the test samples are manufactured within the same batch simultaneously and heat-treated with identical conditions. Heat treatment parameters are supplied by the machine manufacturer as holding at 800°C 2 hours in an argon atmosphere and followed by furnace cooling to room temperature. This stress relief heat treatment was applied because of the thermal residual stress-induced deformations during cutting the part from the build platform [10]. Test specimens were then CNC machined to comply with the corresponding test standards. The optimized part and the witness fatigue test samples were heat-treated with same parameters then Hot Isostatically Pressing (HIP) was conducted for the qualification requirements at 900°C and 1000 Bar. As-built surface properties of L-PBF manufactured part is considered insufficient for a fatigue critical part. To improve the surface properties of the part, chemical and chemical/mechanical polishing processes were applied. After the surface finishing process, the assembly contact interfaces of the part were machined to achieve the required geometrical tolerances.

2.4. Design and Analysis

The flowchart of design, optimization and analysis of the structurally optimized part is presented in Figure 1. Before TO, design and non-design spaces are fully defined. The design volume has been chosen as inclusively as possible to reach the optimum material distribution. Non-design spaces include the assembly interfaces of the application part. And during the modeling the non-design spaces should consider tooling accessibility and the interaction with the other sub-system components. In the optimization process, the prepared design volume was first subjected to finite element analysis according to the loading condition that constitutes the optimization boundary condition. As the solution principle of the Solid Isotropic Material with Penalization (SIMP) method used in topology optimization, an artificial density value was assigned to each finite element and it was decided whether the elements should remain in the de-

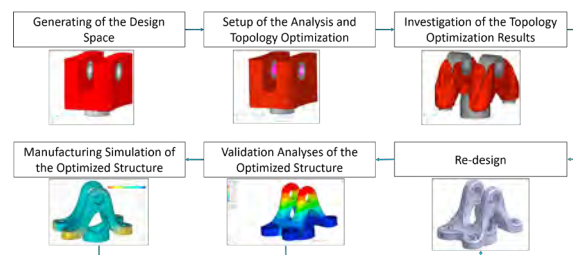


Fig. 1. Design - Optimization Flowchart

sign volume according to the load exposure acquired from the finite element analysis results.

Topology optimization problem used in the design of the aerospace part is :

$$\begin{aligned}
 & \text{Find} && [\rho_1, \rho_2, \dots, \rho_N]^T \\
 & \text{Minimize} && C(\rho) = u^T K(\rho) u \\
 & \text{Subject to} && K(\rho) u = f \\
 & && \sum_{i=1}^N \rho_i v_i - \bar{V} \leq 0 \\
 & && 0 \leq \text{MoS} \\
 & && 0 \leq \rho_{min} \leq \rho \leq 1
 \end{aligned} \tag{1}$$

where ρ is the artificial density vector containing all design variables, C is the compliance of the structure, K is the global stiffness matrix, u is the displacement vector, f is the external force vector, v_i is the volume of each finite element, N is the total number of elements, \bar{V} is the prescribed volume limit value, MoS is the margin of safety and ρ_{min} is a number close to zero to avoid the singularity problem.

The Margin of Safety (MoS) is calculated to ensure the static requirement for the part to be optimized as follows:

$$\text{MoS} = \frac{\sigma_{allowable}}{\sigma_{max} \times SF} - 1 \tag{2}$$

where $\sigma_{allowable}$ is the yield stress of the material, σ_{max} is the von-Mises stress result obtained from FEA and SF is the safety factor that covers AM uncertainties and the deviation based on FEM. The safety factor (SF) is chosen as 2 because the selected additive manufacturing method for the production of the part has higher uncertainties than the conventional manufacturing methods [12].

The resulting isosurface geometry has been remodeled in a CAD environment as a Non-uniform rational B-splines (NURB) surface for validation analysis and manufacturability requirements. The remodeled optimized part was subjected to validation analysis and it was checked if the final geometry meets the mechanical strength criteria. After static analyses, fatigue life calculations were made by analytical method against fatigue loads of the optimized part, which are among the other critical loading conditions. And as the last effort before L-PBF, manufacturing simulations of the final part geometry were carried out with thermo-mechanical analysis, and possible distortion/residual stress conditions were investigated.

3. Results and Discussions

3.1. Topology Optimization

Topology optimization of the selected aircraft part is conducted to obtain a design with maximum available stiffness and 40 % weight reduction of the original part. To start optimization work, the part geometry was split into 2 volumes as design space where topology optimization was performed and non-design space as the unused/kept volume of the part during optimization. These volumes are given in Figure 2. Loading conditions of the fatigue critical part are given as static with pre-loading and cyclic loads and all loading conditions are shared in Table 3. Since both static and fatigue analysis could not be

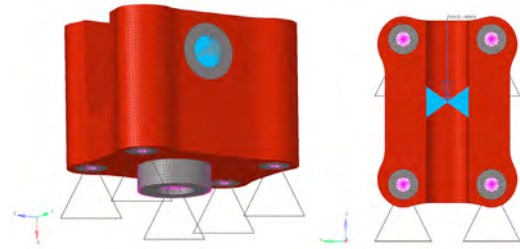


Fig. 2. Topology optimization setup including design space (red region) and non-design space (gray regions)

solved at the same time while topology optimization, -8900 N which is the static load and the maximum loading condition was used during the optimization. In optimization setup, design space was discretized with 238751 finite elements and as seen in Figure 2, it was fixed from connector holes to be analyzed as hard-mounted. Static load was applied to the corresponding region of the structure with RBE3 elements.

As a result of the performed topology optimization in the Altair Optistruct® software, normalized objective function history decreased as 80 % of the initial value of the design space in 17 iterations. According to von-Mises stress results of the final iteration, the MoS value was calculated as nearly 12 using Equation 2 to check the static requirements of the structure and it was found in the feasible region. When the volume constraint function to be needed to satisfy 80 % mass saving of the design space was investigated, it is determined to be found in the feasible region of the optimization problem. To investigate the optimization result and supply reference geometry for the re-design phase, the elements with the design variable below 0.5 were removed from the final design and the reference model was exported as a .stl file (Figure 3).

3.2. Redesign of the Topology Optimization Result

For the manufacturing requirements and validation analyses of the parts designed with topology optimization, the isosurface geometries resulting from the optimization were remodeled as NURB surfaces. This remodeling of the optimized part was performed in a CAD environment with a generative shape design module by taking the stl geometry exported from FEM software. NURB modeling of the isosurface geometry provided more accurate results from the validation analyses and at the same time, it was ensured that the necessary adjustments such

Table 3. Loading conditions of the optimization part

Static Loading Condition		
Load Case	Load (N)	
Static Limit	-8900	
Cyclic Loading Condition		
Load Case	Max Load (N)	Min. Load (N)
HCF	-2234	-335
LCF	-3760	1916

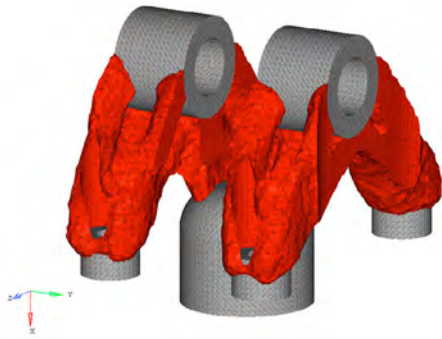


Fig. 3. Topology optimization result

as size change in the part geometry, minor changes in the part feature/section can be made parametrically after the validation analyses. Remodeling of the optimized part and the final manufacturing model is given in Figure 4. Topology optimization and the redesign efforts are considered nearly equal in engineering time and resource usage because in additive manufacturing and conventional manufacturing workflow since the only variable is the manufacturing constraints.

3.3. Validation Analyses

The re-modeled CAD geometries were taken into the FEM environment and analyzed with the identical loading and boundary conditions with the topology optimization setup, and then analytical fatigue life calculations were made for the fatigue loading, which is one of the critical loading conditions of the part. The von-Mises stress criterion was used in the static strength calculation of the part. In other words, the von-Mises stresses in the finite elements used in the analysis are expected to remain below the yield strength of the material. The static finite element analysis setup of the optimized and redesigned part

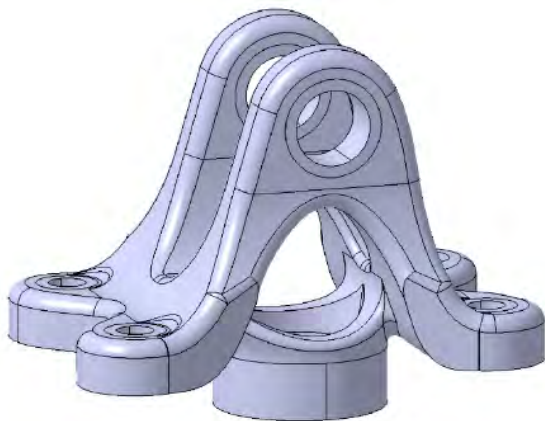


Fig. 4. Final manufacturing design

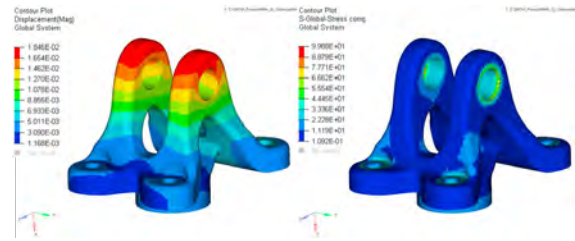


Fig. 5. Static analysis results of optimized part

and the stress and displacement result from the static analysis are given in Figure 5.

In addition to that, it is expected to have an endurance limit greater than 10^7 cycles because the optimized part is a fatigue critical part. For fatigue loads, the optimized part has been subjected to static finite element analysis with loading values at the lower and upper boundaries of the high cycle and low cycle fatigue loads. Static analyses with fatigue loads were performed under the same boundary conditions as topology optimization and static validation analysis setups. Critical stress concentration regions for fatigue damage are determined by experience based on an engineering approach according to load flow conditions. Stress concentration regions where the life calculations were made are given in Figure 6. Maximum principal and signed von-Mises stress data is read from the FE analyses result of the defined stress concentration regions and finite life calculations which are made according to the Soderberg Damage Criterion. In the analytical calculation of the fatigue life of the parts, there are some "endurance limit modifying factors" and these factors define the part by its material, manufacturing, environment, and design specifications. These modifying factors used in the fatigue life calculation are seen in Table 4. Fatigue endurance limit calculation of the optimized part was completed with aforementioned engineering assumptions and fatigue life results are given in Table 5 for each load type and notch region.

3.4. Manufacturing Simulations

After validating the structural properties of the optimized part, L-PBF manufacturing simulations were carried out. These simulations run a thermo-mechanical analysis in the back-

Table 4. Endurance limit modifying factors

Endurance Limit Modifying Factors	Values
Surface Factor, k_a	0.72
Size Factor, k_b	0.90
Loading Factor, k_c	1.00
Temperature Factor, k_d	1.00
Reliability Factor, k_e	0.81
Miscellaneous-Effects Factor, k_{f1} (Region1)	0.68
Miscellaneous-Effects Factor, k_{f2} (Region2)	0.79
Miscellaneous-Effects Factor, k_{f3} (Region3)	0.80
Notch Sensitivity, q	0.38

Table 5. Endurance limit calculations of the optimized part

Loading Type	# of cycles Region #1	# of cycles Region #2	# of cycles Region #3
HCF	2.5×10^{19}	1.3×10^{17}	2.1×10^{15}
LCF	5.1×10^{18}	7.3×10^{12}	1.3×10^{11}

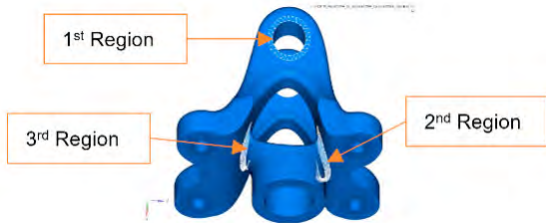


Fig. 6. Critical notch regions for fatigue load

ground, modeling the L-PBF process with the finite element method. For calculation of the thermal distortion and residual stress, some assumptions and simplifications were made to model the problem as accurately as possible while keeping the calculation time and cost relatively low. The predicted heat loss method was used on modeling the heat transfer problem and lattice support structures were homogenized as 3D block elements to lower the uncertainty in the model. Build platform temperature kept constant at 200 °C and it was modeled as an undeformable component. Thermo-mechanical simulations predicted 0,8 mm thermal deformation on the part (see Figure 7). Machining tolerances were expanded to compensate for deformation effects based on the simulation results. Solid metal supports were applied on the region where maximum distortion was expected (See Figure 8).

In these simulations, Autodesk Netfabb® software was used as the thermo-mechanical solver and the solver was validated experimentally with residual stress measurements taken from L-PBF manufactured samples, with XRD and hole-drilling methods. But this experimental validation process kept out of the scope of this article.

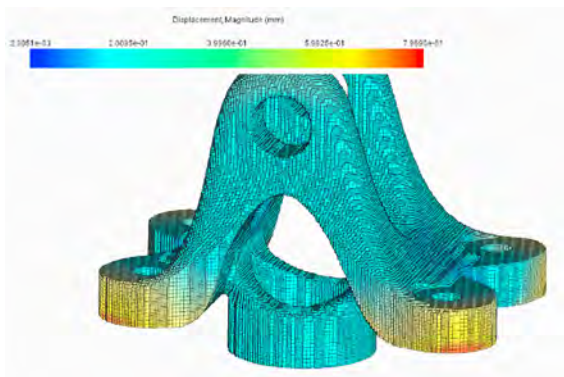


Fig. 7. Displacement results of thermo-mechanical simulation of optimized part

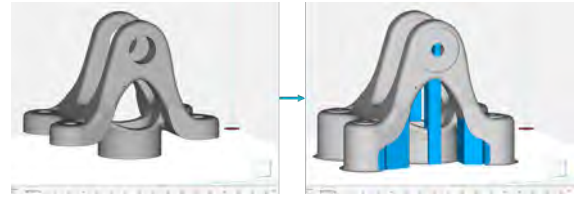


Fig. 8. Generation of manufacturing model

From a time consumption and cost point of view; manufacturing simulations seem like an additional step in the process since in conventional manufacturing of the part, no manufacturing simulation work was conducted. But in the conventional method, the work part is being manufactured with computer numerical control(CNC) machining. Because of that a computer-aided manufacturing(CAM) effort is necessary to create tool-paths and machine algorithms. Moreover, this process takes nearly the same amount of engineering time as the simulation.

3.5. Additive Manufacturing of the Part

Manufacturing of the optimized part was accomplished with the EOSINT M280 L-PBF machine with default processing parameters. Insight of the thermo-mechanical process simulation results of the optimized part, build orientation, and support structure generation efforts were made to achieve successful manufacturing without thermal distortion and cracks. Before the manufacturing phase of the optimized part, to comply with the post-processing requirements, surface tolerances were applied to outer part surfaces and assembly interfaces for chemical and mechanical polishing and also for machining. Integration of support structures and the changes applied for post-process efforts are shown in Figure 8.

After L-PBF manufacturing, the part was heated for thermal stress relieving then cut from the manufacturing table with a wire EDM process. The manufactured part is shown in Figure 9, already connected to the building table.

After cleaning the support structures and removing the excess powder, part and the witness samples were HIPed for a fully dense part. The HIP process is applied at 900 °C and 1000 Bar. The aforementioned surface post-processes were applied after the HIP process. Firstly optimized part was subjected to chemical polishing followed by chemical-mechanical polishing. Chemical and mechanical polishing parameters are not presented because they were not shared by the process vendor.

The original part selected in this study is currently being used in manned aircraft platforms and should comply with the aviation the qualification standards. For that reason, fatigue and static loading tests at qualification level will be conducted on the optimized part with the same configuration used in numerical analyses.

4. Conclusions

In this study, the design of a fatigue-critical aerospace part for additive manufacturing with topology optimization is pre-



Fig. 9. L-PBF Manufactured optimized part

sented. The optimized part was designed 45 % lighter in mass and the mechanical strength requirements of the optimized part were validated by finite element analyses and analytical methods. It was ensured that the part would be manufactured without thermal distortion and in accordance with the subsequent post-processes to be applied with the manufacturing process simulations. The optimized part was successfully manufactured with the L-PBF method and after being subjected to heat treatment, HIP, chemical, and mechanical surface treatments, it was made ready for real condition tests. In summary, the process of developing a fatigue-critical aerospace part with a "design for additive manufacturing" point of view has been proposed comprehensively with a holistic approach that can be used as a guide for AM design-manufacturing-validation workflows.

Acknowledgements

The authors thank the support of Turkish Aerospace under grant project DKTM 2018/05 ongoing with collaboration between Gazi University and Turkish Aerospace.

References

- [1] Bendsøe, M.P., Kikuchi, N., 1988. Generating optimal topologies in structural design using a homogenization method. *Computer Methods in Applied Mechanics and Engineering* 71, 197–224. doi:10.1016/0045-7825(88)90086-2.
- [2] Bendsøe, M.P., Sigmund, O., 2004. *Extensions and applications*. Springer Berlin Heidelberg, Berlin, Heidelberg. pp. 71–158. doi:10.1007/978-3-662-05086-6_2.
- [3] Collet, M., Bruggi, M., Duysinx, P., 2017. Topology optimization for minimum weight with compliance and simplified nominal stress constraints for fatigue resistance. *Structural and Multidisciplinary Optimization* 55. doi:10.1007/s00158-016-1510-6.
- [4] Duysinx, P., Van Mieghroet, L., Lemaire, E., Brülls, O., Bruyneel, M., 2008. Topology and generalized shape optimization: Why stress constraints are so important? *International Journal for Simulation and Multidisciplinary Design Optimization* 2(4) 2. doi:10.1051/ijsmdo/2008034.
- [5] Frazier, W., 2014. Metal additive manufacturing: A review. *Journal of Materials Engineering and Performance* 23. doi:10.1007/s11665-014-0958-z.
- [6] Holmberg, E., Torstenfelt, B., Klarbring, A., 2014. Fatigue constrained topology optimization. *Structural and Multidisciplinary Optimization* 50. doi:10.1007/s00158-014-1054-6.
- [7] Krog, L., Tucker, A., Rollema, G., 2011. Application of topology, sizing and shape optimization methods to optimal design of aircraft components.
- [8] Kumar, J., Nair, C., 2017. Current trends of additive manufacturing in the aerospace industry , 39–54doi:10.1007/978-981-10-0812-2_4.
- [9] Liu, H., Zhang, W., Gao, T., 2015. A comparative study of dynamic analysis methods for structural topology optimization under harmonic force excitations. *Structural and Multidisciplinary Optimization* 51. doi:10.1007/s00158-014-1218-4.
- [10] Mercelis, P., Kruth, J.P., 2006. Residual stresses in selective laser sintering and selective laser melting. *Rapid Prototyping Journal* 12. doi:10.1108/13552540610707013.
- [11] Mierzejewska, , Hudak, R., Sidun, J., 2019. Materials mechanical properties and microstructure of dmls ti6al4v alloy dedicated to biomedical applications. *Materials* 12. doi:10.3390/ma12010176.
- [12] Orme, M., Madera, I., Gschweilt, M., Ferrari, M., 2018. Topology optimization for additive manufacturing as an enabler for light weight flight hardware. *Designs* 2, 51. doi:10.3390/designs2040051.
- [13] Remouchamps, A., Bruyneel, M., Fleury, C., Grihon, S., 2011. Application of a bi-level scheme including topology optimization to the design of an aircraft pylon. *Structural and Multidisciplinary Optimization* 44. doi:10.1007/s00158-011-0682-3.
- [14] Shi, G., Guan, C., Quan, D., Wu, D., Tang, L., Gao, T., 2019. An aerospace bracket designed by thermo-elastic topology optimization and manufactured by additive manufacturing. *Chinese Journal of Aeronautics* 33. doi:10.1016/j.cjja.2019.09.006.
- [15] Sigmund, O., 2007. Morphology-based black and white filters for topology optimization. *Structural and Multidisciplinary Optimization* 33, 401–424. doi:10.1007/s00158-006-0087-x.
- [16] Suresh, S., Lindström, S., Thore, C.J., Klarbring, A., 2021. Topology optimization for transversely isotropic materials with high-cycle fatigue as a constraint. *Structural and Multidisciplinary Optimization* 63. doi:10.1007/s00158-020-02677-2.
- [17] Trivers, N., Carrick, C., Kim, I.Y., 2020. Design optimization of a business aircraft seat considering static and dynamic certification loading and manufacturability. *Structural and Multidisciplinary Optimization* 62. doi:10.1007/s00158-020-02650-z.
- [18] Vatanabe, S., Lippi, T., R. de Lima, C., Paulino, G., Silva, E., 2016. Topology optimization with manufacturing constraints: A unified projection-based approach. *Advances in Engineering Software* 100, 97–112. doi:10.1016/j.advengsoft.2016.07.002.
- [19] Xiong, Y., Yao, S., Zhao, Z.L., Xie, Y., 2019. A new approach to eliminating enclosed voids in topology optimization for additive manufacturing 32, 101006. doi:10.1016/j.addma.2019.101006.
- [20] Zhu, J.H., Zhang, W.H., Xia, L., 2016. Topology optimization in aircraft and aerospace structures design. *Archives of Computational Methods in Engineering* 23, 595–622. doi:10.1007/s11831-015-9151-2.